

## Managing the Power in Smart Grid Management Hybrid Model with MRA in Electric Vehicle System

**B. Gunapriya<sup>1,\*</sup>, N. Samanvita<sup>2</sup>, Thirumalraj Karthikeyan<sup>3</sup>, S. Venkatasubramanian<sup>4</sup>**

<sup>1</sup>Department of Electrical and Electronics Engineering, New Horizon College of Engineering, Bengaluru, Karnataka, India.

<sup>2</sup>Department of Electrical and Electronics Engineering, Nitte Meenakshi Institute of Technology (NMIT), Bengaluru, Karnataka, India.

<sup>3</sup>Department of Artificial Intelligence, Trichy Research Labs, Quest Technologies, Tiruchirappalli, Tamil Nadu, India.

<sup>4</sup>Department of Computer Science and Business Systems, Saranathan College of Engineering, Tiruchirappalli, Tamil Nadu, India.

gunapriyab@newhorizonindia.edu<sup>1</sup>, samanvitha.n@nmit.ac.in<sup>2</sup>, thirumalraj.k@gmail.com<sup>3</sup>, veeyes@saranathan.ac.in<sup>4</sup>

\*Corresponding author

**Abstract:** During times of heavy demand, a Virtual Power Plant (VPP) coordinates power sources, load centres, and energy storage to provide effective power distribution. Mobile robots and electric vehicles (EVs) are essential for maintaining equilibrium between supply and demand. It is still difficult to guarantee a safe connection between end users and VPP aggregators, nevertheless. This study presents a novel method for integrating electric vehicles (EVs) with deep learning algorithms for smart grid power management. The main function of the system is to provide a reliable EV fleet platform by forecasting EV charging trends using SoftMax regression and a deep autoencoder. It was surprising to learn that the eating habits of bottlenose dolphins in the mud rings off the coast of Florida served as inspiration for the deep autoencoders. Inspired by the way dolphins graze on mud rings, the novel Mud Ring Algorithm (MRA) fine-tunes these deep autoencoders for global optimisation. This method outperformed conventional training models, achieving an impressive 98.50% accuracy. This discovery enables strategic power distribution from the EV network as required, reducing power fluctuations and greatly improving smart grid power management. This invention has the potential to improve power grid stability and reliability while optimising EV use.

**Keywords:** Virtual Power Plant; Mud Ring Algorithm; Electric Vehicles; SoftMax Regression; Deep Autoencoder; Smart Grid Management; Power Consumption; Internal Combustion Engine.

**Cite as:** B. Gunapriya, N. Samanvita, T. Karthikeyan, and S. Venkatasubramanian, "Managing the Power in Smart Grid Management Hybrid Model with MRA in Electric Vehicle System," *AVE Trends in Intelligent Energy Letters*, vol. 1, no. 2, pp. 100–114, 2025.

**Journal Homepage:** <https://www.avepubs.com/user/journals/details/ATIEL>

**Received on:** 24/11/2024, **Revised on:** 12/01/2025, **Accepted on:** 01/03/2025, **Published on:** 09/12/2025

**DOI:** <https://doi.org/10.64091/ATIEL.2025.000189>

### 1. Introduction

Electric vehicles (EVs) are becoming increasingly popular among policymakers, researchers, business leaders, and consumers due to growing concerns about the environment and the need for clean energy. One of the best ways to reduce our fuel consumption, cut emissions, and boost energy conversion efficiency is to switch to EVs [1]. The exponential upsurge in the

Copyright © 2025 B. Gunapriya *et al.*, licensed to AVE Trends Publishing Company. This is an open access article distributed under [CC BY-NC-SA 4.0](https://creativecommons.org/licenses/by-nc-sa/4.0/), which allows unlimited use, distribution, and reproduction in any medium with proper attribution.

number of electric vehicles on the road will severely challenge the current power grid. Electric vehicles (EVs) can serve as both regulated loads and distributed energy sources in the power grid, connected to the grid through charging and discharging. Efficient charging and discharging scheduling [2] allow EVs to serve as a flexible load and supply, mitigating the power system's peak-valley load difference and levelling out the load profile. The smart grid with EV integration faces this problem, known as the distributed scheduling mode (DSM) [3]. The use of electric motors to propel vehicles has a deep history that predates the widespread adoption of the internal combustion engine (ICE) [4]. In 1828, a rudimentary but workable electric motor assembly was installed in an automobile and used to power the vehicle for the first time [5].

Since then, until the early 1900s, considerable progress was made worldwide due to the lack of crude oil purifying procedures and the subsequent expansion of internal combustion engine (ICE) vehicles [6]. Conventional (ICE) vehicles were favoured over electric vehicles (EVs) because they were more affordable to fuel. Thus, during the vehicles, however, the costs associated with doing so now exceed the benefits due to rising emissions standards and dwindling crude oil reserves [7]; [8]. Combating environmental, economic, and sustainability issues has prioritised the development and improvement of EV technology [9]. Initially, many were hesitant to choose EVs over ICE vehicles due to concerns about charging-station availability and the limited range between charges. Because of incremental improvements in semiconductor technology, battery technology, efficient motor design, and energy organisation schemes, all the formerly massive problems have been reduced to mere inconveniences but now appear to run [10]. Recent improvements to the grid substructure, including the full implementation of a smart grid (SG) arrangement, have enabled EV integration without noticeable disruptions, both as individual units and as part of coordinated clusters [11]. Power grids can now support more efficient usage patterns and grid services thanks to EVs' unidirectional control and bidirectional flow capabilities [12]; [13]. The following are some of the reasons why EVs should be widely adopted and how they should be used effectively:

- The widespread adoption of electric vehicles offers a practical answer to the problems of global warming, energy insecurity, and the uneven distribution of carbon-based fossil resources.
- Vehicles can stay associated with the grid infrastructure and take part in energy flow programmes by using (ESS) through the vehicle-to-grid (V2G) concept because most vehicles stay parked at their respective grounds of charging substructure for up to 90% of the total time [14].
- Large numbers of EVs can provide backup power during blackouts and provide ancillary services such as peak shaving, voltage and frequency management, and spinning reserve to grid operators.
- When electric vehicles are adopted on a large scale in a technically coordinated and organised fashion, they have a profound impact on the grid, improving performance and efficiency and enabling the mitigation of power quality issues [15].
- By facilitating regulatory operations and system management, EV aggregation can enable consumer participation in the energy market.
- Using various charging topologies, electric vehicles (EVs) can either store excess energy produced by RES for later use or deliver electricity during periods of low generation, thereby smoothing the grid's consumption and supply curves. As a result, EVs could serve as energy buffers between generators and consumers [16].

Distribution system operators (DSOs) can successfully implement DSM programmes with the help of cutting-edge 5G technology, including coordinating EV charging times and pricing tariffs and logging data from the metering substructure [17]. Active consumers in DSM programmes can use one of three practical strategies to alter their energy use habits:

- Load-reduction approaches to lower overall energy consumption; time-of-use adjustments to reduce peak demand.
- The use of sources decreases the reliability of the conventional power grid. All of these methods can be implemented by using electric vehicles as a load alongside energy sources, in a manner analogous to DSM methods.
- By acting as ESSs and providing power during times of need, EVs can reduce grid load.
- They can change how they charge and discharge to help even out demand on the grid.
- They can deliver DSO by providing real-time support when needed and act as bumpers for RES to ensure a steady power supply to the grid [18].
- Customers can be incentivised to reduce their reliance on the utility grid by using different charging tariffs.
- Businesses can gain more from the energy market thanks to a well-coordinated fleet management that streamlines central control and charging for electric vehicles.

Another issue with VPP systems is their lack of cyber-physical security. The weaknesses of traditional centralised control algorithms in smart grids are a major area of study. Researchers have moved on to examining resilience against cyber-attacks as the number of DERs integrated into the power system increases [19]; [20]. However, hostile attackers may still readily tamper with information stored in the VPP's traditional aggregator. Raw data transfer also presents a potential avenue for data leaking. Researchers found no prior studies that concurrently evaluated the role of EVs in projecting energy use and in enabling

efficient computing for local devices. To address these issues, researchers propose a method for integrating electric vehicles into smart grids using deep learning-based artificial intelligence. To begin, researchers present a technique for managing power in VPP that combines deep learning and EV charging prediction. Hybrid is the foundation of the learning process, as it safeguards raw data and enhances communication efficacy. To estimate how much power an EV may deliver when idling to minimise storage during peak load, researchers set up a unique communication method between the aggregator and each EV node, using an AI scheme implemented on programmable hardware (FPGA).

## 2. Related Works

A blockchain-based and AI-driven electrical solution is proposed by Khan et al. [21]. AEBIS is the smart grid platform's vehicle integration solution for managing energy use. The fleet of electric cars is used both as a customer and as a provider of electric energy within a VPP platform, and the solution is built on predictive analytics. The assessment results show that the proposed method generated very accurate predictions of future power usage in the baseline training scenario ( $R^2 = 0.938$ ). The accuracy dropped by 1.7% when a federated learning approach was used. In addition to reducing power fluctuations and providing precise estimates of energy usage, the proposed system also provides a reliable, opportunistic service to transfer excess electricity from the vehicle network. Using a microprocessor with artificial intelligence also ensures financial success. The system's incorporation of blockchain technology enables a secure, transparent service at a cost and with a latency. Tyre pressure monitoring system (TPMS) radio frequency electronic system data protection evaluation provided by Razmjoui et al. [22]. It is shown that it is possible to eavesdrop from a moving automobile at a distance of up to 50 metres. Our inverse study also reveals that messages can be intercepted from considerable distances, posing privacy concerns, as a vehicle's location can be determined by analysing its tyre sensor IDs. Sensor communications can be remotely faked due to the lack of verification in present protocols and the lack of routine message confirmation in-car technology. To enhance TPMS safety, they propose a new, ultra-lightweight mutual authentication mechanism for the TPMS register procedure in the automobile network. Our experiments show that the suggested approach is both efficient and safe for use in TPMS.

TPM virtualisation in a container has been proposed by Cabrera-Gutiérrez et al. [23]. The binaries and libraries housed in the container capacities have various methods in place, such as attestation and sealing, to guarantee their integrity. Containers provide TPM features, including key generation and signing via a RESTful application programming interface. This article proposes an authentication strategy that uses tokens generated by the Web Service to prevent unauthorised access to the container. An industry-relevant use case for microservice-based architecture is proposed: electric car charging stations. The TPM microservice performs the cryptographic processes required for blockchain dealings and stores a copy of the data on the EOS.IO blockchain. The information is accessible via a two-factor authentication system. The virtualised TPM is an example of a microservice that can help address a security concern in a blockchain-based architecture such as this one. Energy trading (ET) schemes for EVs in vehicle-to-everything (V2X) networks have been proposed by Bhattacharya et al. [24]. The EVBlocks system uses a consortium blockchain (CBC) network to provide the safe and reliable transfer of ET data between various organisations, including EVs, CS, and smart grids (SG). There are three stages to the plan's execution. In the first step, researchers investigate an ET service built on a (5G)-capable software-defined networking (SDN) architecture to provide real-time, robust network instrumentation for V2X nodes.

By incorporating SDN into 5G-V2X ecosystems, V2X nodes can eliminate unnecessary go-betweens while still efficiently processing high volumes of queries. The second part introduces a game in which players do not work together to attain a shared goal; instead, they compete to maximise a cost function and eventually reach a Nash equilibrium. Finally, an event-driven scheduling system for EV charging and discharging is presented, along with a Proof-of-Greed (PoG) consensus process to handle these variations. Parameters such as ET time, profitability, computation, and communiqué costs are compared with the acquired findings. Compared to traditional and fixed tariff schemes, EVBlocks' average SOC charge is 22.8 MW, with a high of 377.5 MW, and their average power dissipation is 4.1125 kWh, which is less than 25%. The technique uses a non-cooperative game to converge on stable profit levels for five EVs. The block convergence time for 1000 nodes using the suggested PoG consensus is 138.96 seconds, with a calculation cost of 46.92 ms and a transmission cost of 149 bytes. The analysis demonstrates that the proposed scheme outperforms state-of-the-art methods across the compared parameters. Before joining a VEN, Javed et al. [25] registered with a Registration Authority (RA). As the number of EVs grows, so does the volume of communications, which, in turn, creates data redundancy. Message filtering is used to resolve the matter. The mathematical formulation of VEN delay times is also included in this research. The suggested work also addresses the problem of range anxiety. In addition, a Local Aggregator (LAG) is deployed to validate and control energy trade events. Users are incentivised to join the proposed network in several ways. The suggested model is analysed for security flaws using the Oyente tool and subjected to tests simulating a selfish mining attack.

The simulation findings demonstrate that the proposed research is superior in its ability to provide an EV energy trading and data-sharing system that is safe, efficient, and well-coordinated. The results demonstrate that with the right planning, the danger may be cut by a quarter to a third. Less redundant data storage is also associated with a 40-50% reduction in processing time. One solution proposed by Akhter et al. [26] is to use a blockchain-based management system to unify a network of nodes and

charging stations, with the blockchain verifying the legitimacy of charging stations and the people who charge at them. To further guarantee the safety, honesty, openness, and immutability of transactions, a cryptocurrency-based payment mechanism has also been proposed. To keep up the high standard of service, a reputation management system is used. High-powered miners, assisted by strategically placed edge servers, are used to minimise block generation delays. The suggested system is a virtual machine-based implementation. This paper presents a theoretical examination of the system's feasibility and potential implementation costs. A blockchain-based charging reservation method for electric vehicles with optimal pricing has been proposed by Tanwar et al. [27]. The primary goal is to ensure the safety of information sent between EVs and charging stations. It uses the same communication channel as 5G to guarantee record-breaking low latency and a sky-high level of reliability. To further maximise benefits for everybody involved, the proposed concept employs a double-auction procedure for EVs and charging stations. To gauge how well the suggested method performs, it is compared with established networks such as 4G and LTE-A. Electric vehicle profit and loss, scalability, data storage costs, communication overhead, and data transaction costs are all considered as performance metrics. Compared with conventional methods, the outcomes demonstrate that the proposed strategy is safe and yields the best financial returns for EVs and charging stations.

### 3. Proposed Model

In this paper, researchers zero in on two primary concerns: Two key innovations here are 1) facilitating dialogue between the distributed VPP collector and EV fleets, where DL training for battery-operated charge prediction may take place, and 2) supplanting the traditional VPP aggregator with a deep learning network that is optimised for this task. The client-side EVs' anticipated next-period power consumption is calculated using an artificial intelligence system based on programmable hardware (FPGA). Therefore, researchers can regulate EVs to supply (discharge) based on the EV's remaining power and the power grid's demand. In times of low grid power, the aggregator and its customers can work together to estimate the amount of electricity needed.

#### 3.1. EV Battery Power Consumption Prediction

Accurate and timely energy management necessitates knowing the predicted remaining electricity at each EV node. Factors such as climate, vehicle make and model, driving habits, and geographical location all affect an electric car's actual energy needs [28]. A fully connected neural network predicts power usage given all input features. In Section 4, researchers will deliver the experimental particulars of the predicted power usage.

#### 3.2. EV Battery Charge Mechanism

When there is no request for electricity from the electrical grid, the battery can be charged. Predicting the EV fleet's delivery to the grid is thus the primary objective. The suggested algorithm determines how much electricity each EV should feed back into the grid during peak demand. Starting with each vehicle's maximum battery capacity and its current state of charge (SoC), the residual power is determined. The leftover power is then compared with the predicted power use established in Section 3.1. It cannot provide the electricity at this time if the residual power is less than the anticipated demand or if the EV is on its way. Therefore, the value of E available (the maximum amount of power the EV can supply) is zero. Still, the residual juice might be of use to the next driver when they book. If, on the other hand, the car is plugged in and will remain there until the next billing cycle, the available energy is determined by:

$$E^{\text{available}} = RP - ECP \quad (1)$$

where RP signifies the residual power, and ECP signifies the predictable spent power. At this stage, researchers know how much juice each electric vehicle (hence referred to as "EV") in the fleet has left.  $\{E_i^{\text{available}}\}_{i \in \mathbb{R}^N}$  where I is the vehicle's ID, and N is the total number of EVs. Simply labelling the overall power output of the EV fleet as the sum of  $\{E_i^{\text{available}}\}_{i \in \mathbb{R}^N}$ :

$$E^{\text{supply}} = \sum_{i=1}^N E_i^{\text{available}} \quad (2)$$

The quantity of power the grid should request can then be determined using a decision rule. A parameter denotes each EV's discharge rate. A request is issued to the EV fleet whenever there is an excess (EEL) on the grid's side. If  $E^{\text{supply}} \leq EEL$ , then the discharge rate is set to 100% because all remaining power is needed to mitigate the power shortfall. If  $E^{\text{supply}} > EEL$ , This indicates that the fleet of electric vehicles does not need to supply all of the electricity needed by the facility. The share of the market will be:

$$\rho = EEL/E^{\text{supply}} \quad (3)$$

Once the available power is multiplied by the discharge rate, the total electrical discharge for each EV may be calculated:

$$E_i^{\text{discharge}} = \rho \times E_i^{\text{available}} \quad (4)$$

### 3.3. DL-Based Framework

The network model is responsible for gathering the EV nodes' submitted data sets and carrying out the training process. However, there is significant communication overhead and the risk of data leakage due to the constant flow of raw data. Each EV node communicates with the aggregator to exchange and enhance its local model, a solution enabled by the deep learning (DL) architecture. The entire process consists of a series of training iterations that converge. The following four actions make up the bulk of each round:

$$\nabla_{g_L} = \frac{\delta E(W)}{\delta W} \quad (5)$$

where  $W$  is the weight set and  $E(W)$  is the loss function on  $W$  [29]. The model error is quantified by  $E(W)$ , and the best possible answer can be found using it. Furthermore, denotes partial derivatives:

- Each client sends its local gradients to the aggregator.
- Thirdly, a global gradient is generated by aggregating local gradients.  $\nabla_{g_G}$
- The parameters are updated after the edge nodes have received the global incline from the server site.

$$\nabla_{g_G} = \frac{1}{n} \sum_{i=1}^n \nabla_{g_L}^i \quad (6)$$

$$W^{r+1} = W^r - \eta \nabla_{g_G} \quad (7)$$

$$b^{r+1} = b^r - \eta \nabla_{g_G} \quad (8)$$

Where  $W^r$  and  $b^r$  represent the weights and biases used in the  $r$ th training iteration. Where is the pace of learning?

### 3.4. Proposed DNN-Hybrid Deep Autoencoder Network

At the beginning of this study, features were extracted from a DNN trained directly. The final layer of the DNN is replaced with the bottleneck layer. Low-dimensional nonlinear transformations of the input topographies are what the bottleneck features will explain. The DNN mediates between raw auditory data and refined phonetic characteristics at the output. Researchers employ neural networks (BN-DNNs), in which the DNN's bottleneck layer extracts features. At first, a deep autoencoder network is used to determine which feature is most effective. To further improve the suggested model, a combination of the best feature and additional characteristics has been examined. Using the MRA, the network's weights are optimised as a whole. Expression characteristics are simultaneously categorised using the SoftMax regression method. To identify EV usage, a SoftMax regression autoencoding network is proposed here.

#### 3.4.1. DNN-Aided Bottleneck Feature Extraction

Typically, the features are created, and the fewest neurons in the layer are inserted into the DNN using a specifically constructed DNN. The linear outputs of the neurons in the bottleneck layer were used to obtain bottleneck (BN) characteristics across three distinct layers. Compared with other common characteristics, bottleneck features far outperform the competition. Extraction of BN features is performed using a wide variety of raw characteristics. The bottleneck layer has far fewer neurons for BN feature extraction than other hidden layers. The activation signals in the BN layer are triggered during DNN training, resulting in a compact, low-dimensional representation of the original inputs. Figure 1 provides a high-level perspective of BN feature extraction using DNN. First, EV features are input on the input layer, and then BN features, and the BN layer in particular, are recovered from the DNN's hidden layers. The input, hidden, BN, and output layers (NI, NH, NB, and NO) form the neural network's layered structure. The suggested hybrid LID modelling method uses BN-DNN to extract the bottleneck feature. In this experiment, researchers use the BN-DNN approach, which consists of three hidden layers, the last of which serves as the BN layer, to extract bottleneck features. The DNN is fed a 35-dimensional stacked feature collection, from which it generates a 10-dimensional bottleneck feature. During language recognition, the retrieved bottleneck feature is used.

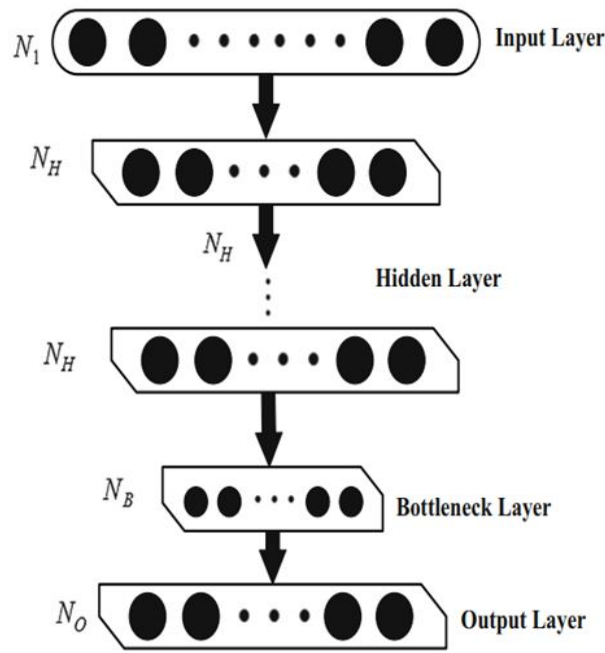


**Figure 1:** Architecture of DNN for feature extraction

### 3.4.2. Deep Autoencoder Network

In this part, researchers focus on detailing the deep regression hybrid model used for language recognition. The deep autoencoder network can identify key characteristics that set each language apart. In this case, researchers use previously learned parameters to define the input vector  $x_i$  ( $1, 2, \dots, N$ ) and the hidden-layer representation  $h_i$ . The joint is computed from the input vector  $x_i$ . It is used as the initial matrix weight. Probability approximation is given by:

$$p(h_i = 1|x) = \sigma(b_i + \sum_j w_{ij}x_j) \quad (9)$$

where  $\sigma$  is the sigmoid role. The sigmoid function is distinct as shadows:

$$\sigma = \frac{1}{1+e^{-z}} \quad (10)$$

The input information to the network is given as  $z$ , and the output statistics of the system are given as  $h_{w,b}(z)$ , and  $w_{ij}$  ( $i, j = 1, 2, \dots, N$ ) designates the original data  $z$  is activated via the charting purpose to deliver  $m_f$  as shadows:

$$m_f = \text{sigm}(w_i z + b_j) \quad (11)$$

Where  $\text{sigm}$  is a known sigmoid function:

$$\text{sigm} = \frac{1}{1+e^{-z}} \quad (12)$$

The rebuilt signal throughout the decoding stage is signified by:

$$\hat{x}_i = h_{w,d}(z) = g(w_i^t m_f + b_{i+1}) \quad (13)$$

The weight matrix  $w$  and the bias between the layers  $b$  are given in the preceding equation. One of the crucial prerequisites of an autoencoder is that the error incurred during renovation be represented by a likelihood function that depends on the output features  $x$ , acquired after data  $x$  is indoctrinated:

$$L(x, \hat{x}) = 1/2 |x_i - \hat{x}_i|^2 \quad (14)$$

### 3.4.3. SoftMax Regression Model

These days, it seems like wherever you look, there's a multiclass classification challenge. At this point in the process, the class label often involves more than two discrete outcomes. The regression, often known as SoftMax regression, is widely used in

practice due to its ease of use and effectiveness [30].  $D = \{(z^{(1)}, y^{(1)}), \dots, (z^{(n)}, y^{(n)})\}$  be the training set,  $z^{(i)}$  ( $i \in \{1, 2, \dots, n\}$ ) signifies the training data, and  $y^{(k)}$  ( $k \in \{1, 2, \dots, m\}$ ) indicates the label of training data. To calculate the posterior probability of a given test case  $z$ ,  $p(y = k|z)$ , the SoftMax regression classifier is presented in Figure 2.

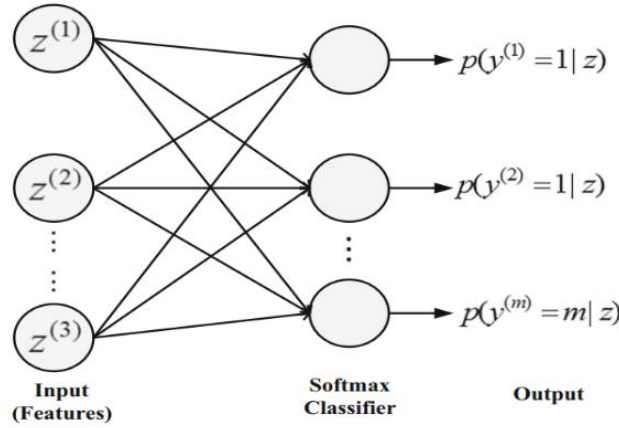


Figure 2: Model of SoftMax regression

#### 3.4.4. Hyper-Parameter Tuning using Mud Ring Algorithm (MRA)

The Mud Ring Algorithm (MRA) simulates a pod of dolphins' entire feeding process, from echolocation to find food to the eventual construction of the mud ring. The approach requires modifying the population size and the number of repetitions, and the initial answer is updated in a single phase using a single equation. It is superior to other optimisation procedures in terms of computational ease, runtime, and convergence speed. As a result, metaheuristics-based MRA is considered. This method effectively obtains the global or near-global optimal solution within a given set of constraints. Therefore, the Jaya technique is used to select optimal weights for the HDAE network in this study. The algorithm interprets the input population as the weights for the hidden layer. Before researchers can perform a mathematical simulation of the MRA method, a few details need to be clarified. Predator-prey interactions and mud-ring feeding are modelled mathematically here. Next, the core operations of the MRA may be described using the pseudocode shown in Algorithm 1.

##### 3.4.4.1. Searching for Prey (Foraging) - Exploration Stage

The following guidelines are used to idealise certain aspects of dolphins' echolocation: All dolphins use echolocation to gauge distance when hunting; dolphins swim at random, employing velocities  $V$  at places  $D$  with a  $K$  to locate prey. While there are likely many factors at play, researchers assume that a dolphin's produced sound volume changes in response to a time step and a pulse rate 'r' that varies from 0 to 1, where 0 denotes no release pulses and 1 denotes the highest pulse release rate. The  $K$  vector has been calculated as:

$$\vec{K} = 2\vec{a} \cdot \vec{r} - \vec{a} \quad (15)$$

where  $\vec{r}$  is a random vector among 0 and 1, and:

$$\vec{a} = 2 \left( 1 - \frac{t}{T_{max}} \right) \quad (16)$$

Researchers use artificial dolphins to look for food (exploration). Dolphins randomly choose a search location in space based on their positional relationships to one another. Therefore, researchers use a random variable  $K$  with values more than 1 or less than 1 to cause the dolphins to search in different directions for the healthiest prey. As a result, a random dolphin is picked rather than the best dolphin. The MRA method can perform a global search thanks to the selection mechanism and the constraint  $|K| = 1$ . The MRA process is described mathematically as follows. Researchers need to specify when and how the coordinates and velocities will be refreshed. At each discrete time  $t$ , the practicability  $D^t$  is calculated from the velocity  $V^t$ :

$$\vec{D}^t = \vec{D}^{t-1} + \vec{V}^t \quad (17)$$

where  $V$  is reset as a random vector. Originally, each dolphin is assigned an accidental velocity from  $[V_{min}, V_{max}]$  that is designated contingent problematic of interest.

### 3.4.4.2. Mud Ring Feeding- Exploitation Stage

Once dolphins have located their target, they can close in on it. Since the position of the space is, the MRA approach treats the target prey (optimal or near it) as the best key at the moment. Once the agent has been found, the additional locations match the finest dolphin site. The subsequent equations characterise this pattern:

$$\vec{A} = |\vec{C}\vec{D}^{*t-1} - \vec{D}^{t-1}| \quad (18)$$

$$\vec{D}^t = \vec{D}^{*t-1} \cdot \sin(2\pi l) - \vec{K} \cdot \vec{A} \quad (19)$$

Where  $D^*$  is the best site the dolphin has ever been in. Every time a better position becomes available,  $D^*$  should be updated. While the prey, the finest dolphin, travels in a circle, waving its tail quickly in the sand to create the pattern of a sine wave and producing a plume. The following is the formula for determining the vector  $C$ :

$$:\vec{C} = 2 \cdot \vec{r} \quad (20)$$

The search space can be navigated to any coordinate by calculating a random vector,  $r$ . In this way, any dolphin may use Eq. (20) to explain its position near the optimal one by simulating the prey's encirclement. MRA begins its search given a pool of potential answers (current dolphin locations). Dolphins protect their positions based on the best site found so far or a randomly chosen dolphin at each time step. To switch between exploration and exploitation, a parameter is dependent on the time step. To defend their respective places, dolphins are chosen at random until  $|K| \geq 1$ , in which case the best possible dolphin is chosen. Keep in mind that there are only two fixed parameters ( $C$  and  $K$ ) in the MRA procedure.

Algorithm 1:

MRA Algorithm

Set the Initial Population of Dolphins

Randomly,  $D_i, i \in [1, 2, \dots, n]$  and Velocity  $v_i$

Calculate the Fitness Function of Each Dolphin

$D^*$  = the Best Dolphin Position

While ( $t < T_{max}$ )

for  $i=1$  to  $n$

Modify  $K, C, a$ , and  $l$

if  $|K| \geq 1$  Then

Generate New Solutions by Modifying

Velocity  $v_i$  using Eq. (18)

Else

/\* Forming the Mud ring\*/

Update the Current Dolphin Location

Using Eq. (20)

end If

end for

Update the Bounds for Dolphin Outside

the Search Space

Attain the Dolphin's Fitness Functions

Update  $D^*$  in Case of a Better Position

Existence

Set  $t \rightarrow t+1$

end While

Return  $D^*$  (the best position)

### 3.5. The Hybrid Perfect of SoftMax Regression

This section details the hybrid SoftMax regression used for EV charging prediction. When given a set of parameters, a deep autoencoder will find characteristics that help distinguish between them. To approximate the posterior probability for each language and achieve ultimate accuracy with MRA, the hybrid model can be observed to fully link the DAE with SoftMax regression as a soft hybrid. To verify the accuracy of our hybrid DAE model, researchers consider five levels during the identification phase: one input and one output layer, and five hidden layers. During training and fine-tuning, HDAE receives a set of feature combinations and estimates a single probability score for all possible permutations of feature descriptors. The SoftMax regression is assigned to the EV charging demand problem as the output layer of a DAE (autoencoder). Training is the most important stage of DAE, as discussed in Section. 3.4.2. After that, researchers use MRA to fine-tune the network's overall parameters by starting the back-propagation process. The number of layers can be denoted by  $l$ , and the goal function can be written as:

$$s(w_l, w_{i,k}|_{k=1}^{l-1}, b_{i,k}|_{k=1}^{l-1}) = \arg \min_{w_l, w_{i,k}, b_{i,k}} \frac{1}{2N} \sum_{i=1}^N |y_i - g_l(f_l(h_i^{l-1}))|^2 \quad (21)$$

where the activation charge of the hidden layer  $(l-1)$  th is represented as  $h_i^{l-1} = f_{l-1}(f_{l-2}(\dots f_1(x_i)))$ , the label of  $x_i$  is symbolised as  $y_i$ , the weight of the concluding layer is represented as  $w_l$ , and the layer is signified as  $b_{i,k}$  and  $w_{i,k}$ . Furthermore, the parameters of DAE were efficiently determined:

$$w_l := w_l + \Delta w_l = w_l - \mu d^l h^{l-1} \quad (22)$$

$$w_{1,k} := w_{1,k} + \Delta w_{1,k} = w_{1,k} - \mu d^k h^{k-1} \quad (23)$$

$$b_{1,k} := b_{1,k} + \Delta b_{1,k} = b_{1,k} - \mu \sum_{j=1}^R d^k \quad (24)$$

where  $d^l = (h^l - Y)h^l(1 - h)$ ,  $d^k = w_{k1}^t d^{k+1}(1 - h^k)$  (when  $k < l$ ), The learning proportion is designated as  $\mu$  and characterised as  $R$ . Until the goal function reaches the max epoch,  $w_{1,k}$  and  $b_{1,k}$  are iterated. When training a DAE model, it is necessary to find the weight parameters that minimise the objective function (21), and MRA is the technique of choice.

## 4. Results and Discussion

Features of weather, topography, and user information were previously discussed and are included in the data set used to anticipate energy usage. Researchers gathered data on the climate in the Fukushima, Kanagawa, and Tokyo metropolitan areas of Japan [2] between January 2020 and July 2020. The reservation began between 00:00 and 23:00 and ended at any time between 0 and 24 hours later. Researchers considered the minimum and maximum ages for drivers specified by the Class 2 licence [2]. Using the input features and the measurement methodology, the daily power consumption was calculated. The data can be downloaded from [31]-[33]. Table 1 summarises the dataset's specifics.

**Table 1:** Data energy consumption set for the vehicle

Input Feature	Unit and Datatype	Value
Start time	Int	0 to 23
Longitude	m/s, Float	139.09 to 139.76
Gender	Male/Female, Int	0 to 1
Age	Year-old, Int	21 to 69
Duration of use	Hours, Float	0 to 24
Weekday	Mon.to Sun., Int	1 to 7
Temperature	$^{\circ}C$ , Float	-11.61 to 33.83
Rainfall	mm, Float	0 to 19.04

Humidity	%, Float	0.07 to 1
Wind Speed	<i>m/s</i> , Float	0.24 to 23.45
Latitude	<i>m/s</i> , Float	35.15 to 37.29
<b>Output</b>	<b>Unit and Datatype</b>	<b>value</b>
Power consumption	<i>KWh</i> , Float	0 to 140

Independent and identically distributed (IID) data from each customer were used in the analysis. Researchers split the full dataset across three clients, each receiving a subset of 1,000 randomly generated samples. In most situations, however, the resident data on each EV node is not IID, since it was collected at different times or by different drivers. As a result, researchers examined how using non-IID data distributions affected the results. One particularly intriguing scenario involves multiple reservations for the same EV at different times of day. Researchers considered a group of four customers, one for each hour: 6:00-11:59, 12:00-17:59, 18:00-23:59, and 0:00-5:59. They were also curious about what might happen if people of different ages made reservations for the EVs. There are a total of five customers in this instance, spanning the ages of 21 to 29, 30 to 39, 40 to 49, 50 to 59, and 60 to 69. Fifty iterations of the simulation were performed for each DL training. The model's efficacy was evaluated using the R<sup>2</sup> score. Data was stored and disseminated using the Swarm platform. Our testing platform was Ubuntu 18.04.3. Information on various crucial factors is stored in a genesis file that contains the full setup of early conditions. The resulting confusion matrix, displayed in Table 1, is based on this value. In this context, the four most important terms in the confusion matrix are true positive (TP), true negative (TN), false positive (FP), and false negative (FN).

**Table 2:** Confusion matrix

Actual Lecture	Predicted Lecture	
	Positive	Negative
Positive	<i>Ap</i>	<i>Bn</i>
Negative	<i>Bp</i>	<i>An</i>

In this research, researchers examine the effectiveness of many popular categorisation performance algorithms using the criteria listed in Table 2:

$$\text{Accuracy} = (Ap + An)/(Ap + Bp + An + Bn) \quad (25)$$

$$\text{Recall(or Sensitive or True Positive rate)} = Ap/(Ap + Bn) \quad (26)$$

$$\text{Precision} = Ap/(Ap + Bp) \quad (27)$$

$$\text{F1 - Measure} = 2 \frac{\text{Precision} \times \text{Recall}}{\text{Precision} + \text{Recall}} \quad (28)$$

$$\text{False Positive rate (FPR)} = Bp/(Bp + An) \quad (29)$$

As a result, researchers also use the TPR to the FPR at multiple thresholds. AUC is preferred over accuracy as a performance metric because it is not dependent on the threshold value. When the AUC reaches 1, the model's overall performance is optimal.

**Table 3:** Analysis of proposed DL without MRA

Classification	F1-Measure	Precision	AUC	Recall	Accuracy
RNN	0.323	34.94	0.958	30.97	94.03
CNN	0.340	34.25	0.957	32.06	95.24
MLP	0.282	28.02	0.929	28.40	93.80
AE	0.257	29.79	0.929	22.62	94.10
DBN	0.311	29.56	0.935	32.82	93.90
<b>Hybrid model</b>	0.378	36.82	0.966	39.19	97.27

The proposed DL without MRA analysis is shown in the third edition of Table 3 above. The MLP model's performance in the analysis yielded an AUC of 0.92, F1-Measure of 0.282, precision of 28.02, recall of 28.40, and accuracy of 93.80. Another AE model also achieved an AUC of 0.929, F1-Measure of 0.257, recall of 29.79, and accuracy of 94.10, all within the respective ranges. Another DBN model also achieved an AUC of 0.935, an F1-Measure of 0.311, a precision of 29.56, a recall of 32.82,

and an accuracy of 93.90, all measured in their respective terms. Another RNN model also achieved an AUC of 0.958, an F1-Measure of 0.323, a precision of 34.94, a recall of 30.97, and an accuracy of 94.03, all measured separately. Another CNN model achieved the following results: an AUC of 0.957, an F1-Measure of 0.340, precision values of 34.25 and 32.06, recall values of 32.06, and accuracy of 95.24, all in that order. The AUC of another hybrid model was 0.966, the F1-Measure was 0.378, the precision was 36.82, the recall was 39.19, and the accuracy was 97.27, all of which were achieved in that order.

**Table 4:** Comparative investigation of projected DL with MRA

Classification	Accuracy	F1-Measure	Precision	Recall	AUC
RNN	96.78	0.548	58.60	52.02	0.976
MLP	94.44	0.418	41.44	41.89	0.936
AE	94.50	0.358	40.10	33.01	0.941
DBN	95.89	0.437	44.59	41.98	0.949
CNN	97.26	0.518	55.74	50.62	0.968
<b>Hybrid model</b>	<b>98.50</b>	<b>0.600</b>	<b>62.34</b>	<b>58.08</b>	<b>0.981</b>

The Analysis of the comparative investigation of the proposed DL with MRA is shown in Table 4 above. The MLP model's performance in the analysis resulted in AUC values of 0.936, 0.418 for F1-Measure, 41.44 for precision, 41.89 for recall, and 94.44 for accuracy, respectively (Figure 3).

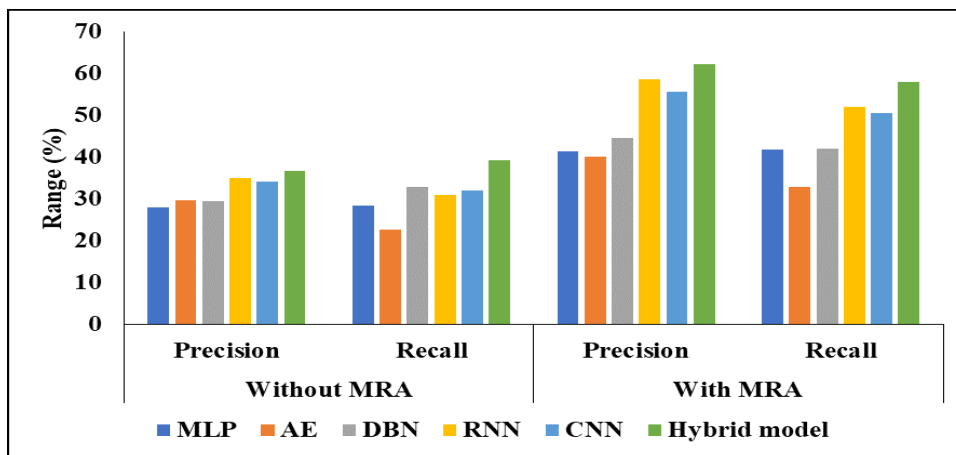


**Figure 3:** Comparative analysis of different models

Another AE model also achieved an AUC of 0.941, F1-Measure of 0.358, precision of 40.10, recall of 33.01, and accuracy of 94.50, all in accordance with the data (Figure 4).

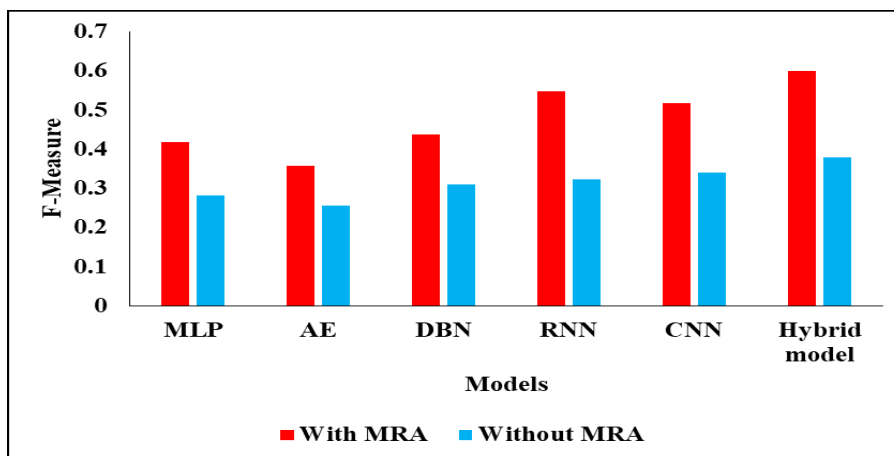


**Figure 4:** F1-measure analysis by using the proposed model

Another DBN model also achieved an AUC of 0.949, F1-Measure of 0.437, precision of 44.59, recall of 41.98, and accuracy of 95.89, all within their respective ranges. Another RNN model achieved the following AUC, F1-Measure, precision, recall, and accuracy values, in that order: 0.976 for AUC, 0.548 for F1-Measure, 58.60 for precision, 52.02 for recall, and 96.78 for accuracy (Figure 5).

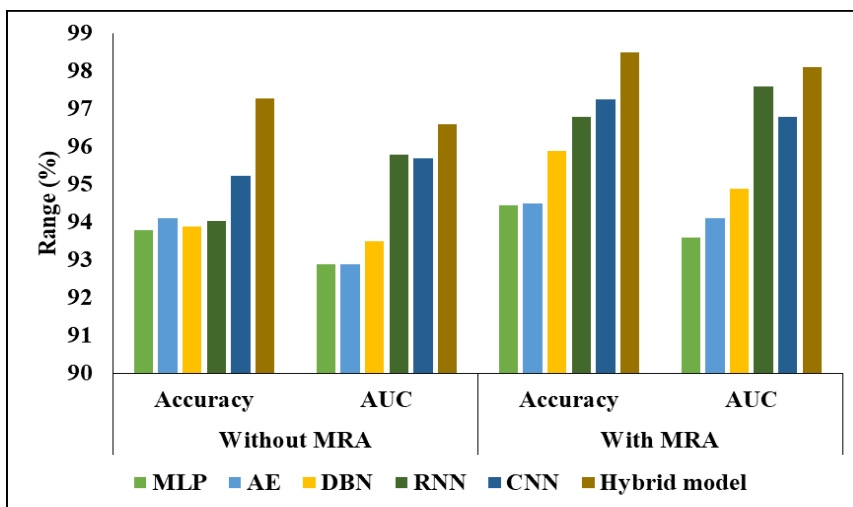


**Figure 5:** Graphical representation of the proposed model with various DL models

Another CNN model achieved the following results: AUC of 0.968, F1-Measure of 0.518, precision of 55.74, recall of 50.62, and final accuracy of 97.26. Another hybrid model achieved an AUC of 0.981, F1-Measure of 0.600, precision of 62.34, recall of 58.08, and accuracy of 98.50, respectively.

**Table 5:** Existing models comparison

Classification	Accuracy	F1-Measure	Precision	Recall	AUC
Robust Controller Model	98	-	-	-	-
Multi-Method Fusion of Big Data Model	91.82	-	-	-	-
YOLO-V4 model	95.34	-	-	-	-
Hybrid model	98.50	0.600	62.34	58.08	0.981

According to Table 5 and Figure 6, the Robust Controller Model had an Accuracy of 98%, the multi-method fusion of Big data model had an Accuracy of 91.82%, and the YOLO-V4 model had an Accuracy of 95.34%.

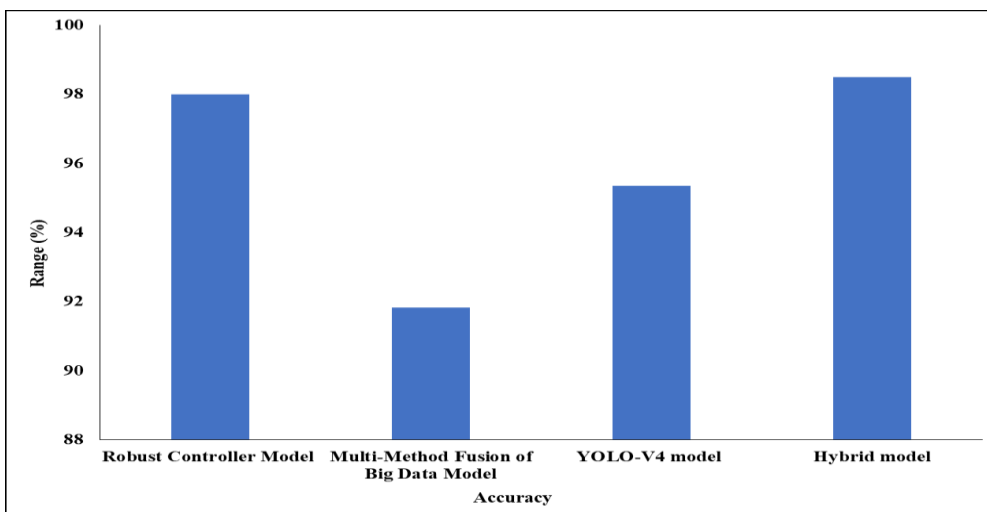


**Figure 6:** Accuracy comparison of existing models

The suggested hybrid model got an Accuracy of 98.50%, an F1-measure of 0.600, a Precision of 62.34%, a Recall of 58.08%, and an AUC of 0.981. The proposed hybrid model surpasses all other models in accuracy when applied to the provided dataset.

## 5. Discussion

In the preceding section, researchers compared several deep learning architectures. The suggested method delivers superior performance with much less overall training and communication time than the standard learning arrangement, which requires raw data exchange among clients. Time and money savings can be maximised by evaluating hardware complexity. The proposed paradigm effectively addresses issues arising from non-IID distributed data and partial device involvement. In addition, the technique through which models may be exchanged without disclosing the underlying data set is seen as a means of safeguarding users' right to privacy. Our DL-based network accurately predicted EV power usage, which is useful for planning future electricity supply or reserving EVs. But there are still risks because of rogue clients and hijacking. There are still many obstacles that the decentralised design must overcome. Due to the massive memory needs and sluggish transaction or mining pace, system performance will degrade as the number of blocks increases. There is an additional burden on the system since the very first models are always kept in the network.

## 6. Conclusion

In this study, researchers present an innovative deep learning-based solution for smart grid power management that seamlessly incorporates electric vehicles (EVs) into the energy ecosystem. The proposed method was developed by carefully examining the computational and physical fundamentals required for smart grids to manage energy efficiently and intelligently. Our system emphasises quick, accurate energy monitoring, enabling real-time decision-making and more efficient use of power resources. The results show that faster energy monitoring and control greatly improve the stability and performance of the whole system. Also, accurate predictions of electricity demand are very important for the car-sharing industry, as they provide key information for organising reservations, predicting vehicle availability, and creating optimal charging schedules. These features help make EV-based mobility services more reliable and happier customers. The proposed deep learning architecture is designed to preserve users' private and rare data while accelerating learning. The model performs almost as well as typical deep learning methods, despite being quite lightweight. Training is done on an artificial intelligence processor with low latency and low power to make things even more efficient. This hardware alternative uses less energy, costs less overall, and makes the solution easier to move and use in the real world. Deep learning networks that are already available do offer open and secure services. Still, they usually require a lot of processing power and storage space, making it hard to scale them up. Our method addresses these problems by reducing resource requirements without sacrificing accuracy or reliability. Because of this, the proposed system is well-suited for future smart grid applications. Future work will focus on improving the network's communication system so it can be deployed more quickly, scaled up, and respond in real time in large-scale smart grid settings.

**Acknowledgement:** The authors sincerely acknowledge the academic support and research environment provided by New Horizon College of Engineering, Nitte Meenakshi Institute of Technology (NMIT), Saranathan College of Engineering, and Quest Technologies.

**Data Availability Statement:** The research is based on datasets involving URL data and smart grid management using a hybrid MRA approach for electric vehicle systems. The authors collaboratively analysed these datasets and are available upon request from the corresponding author.

**Funding Statement:** This research and manuscript were completed without receiving financial support from any funding agency or organisation.

**Conflicts of Interest Statement:** The authors declare that there are no conflicts of interest associated with this work. All sources of information have been appropriately cited and referenced.

**Ethics and Consent Statement:** Ethical approval was obtained prior to the study, and informed consent was secured from all participating organizations and individuals involved in the data collection process.

## References

1. X. Zhang, C. Liu, K. K. Chai, and S. Poslad, "A privacy-preserving consensus mechanism for an electric vehicle charging scheme," *J. Netw. Comput. Appl.*, vol. 174, no. 1, p. 102908, 2021.
2. Z. Wang, M. Ogbodo, H. Huang, C. Qiu, M. Hisada, and A. B. Abdallah, "AEBIS: AI-Enabled Blockchain-Based Electric Vehicle Integration System for Power Management in Smart Grid Platform," in *IEEE Access*, vol. 8, no. 12, pp. 226409-226421, 2020.

3. N. T. Mbungu, A. A. Ismail, R. C. Bansal, A. K. Hamid, and R. M. Naidoo, "An optimal energy management scheme of a vehicle to home," *IEEE 21st Mediterranean Electrotechnical Conference (MELECON)*, Palermo, Italy, 2022.
4. S. Rehman, A. B. Mohammed, L. Alhems, and F. Alsulaiman, "Comparative study of regular and smart grids with PV for electrification of an academic campus with EV charging," *Environ. Sci. Pollut. Res.*, vol. 30, no. 31, pp. 77593–77604, 2023.
5. A. Miglani, N. Kumar, V. Chamola, and S. Zeadally, "Blockchain for Internet of Energy management: Review, solutions, and challenges," *Comput. Commun.*, vol. 151, no. 2, pp. 395–418, 2020.
6. G. A. Salvatti, E. G. Carati, R. Cardoso, J. P. da Costa, and C. M. D. O. Stein, "Electric vehicles energy management with V2G/G2V multifactor optimisation of smart grids," *Energies*, vol. 13, no. 5, p. 1191, 2020.
7. Y. Li, Z. Ni, T. Zhao, T. Zhong, Y. Liu, and L. Wu, "Supply function game-based energy management between electric vehicle charging stations and electricity distribution systems considering quality of service," *IEEE Trans. Ind. Appl.*, vol. 56, no. 5, pp. 5932–5943, 2020.
8. Y. Wu, Z. Wang, Y. Huangfu, A. Ravey, D. Chrenko, and F. Gao, "Hierarchical operation of electric vehicle charging station in smart grid integration applications—An overview," *Int. J. Electr. Power Energy Syst.*, vol. 139, no. 7, p. 108005, 2022.
9. V. T. Tran, M. R. Islam, K. M. Muttaqi, and D. Sutanto, "An efficient energy management approach for a solar-powered EV battery charging facility to support distribution grids," *IEEE Trans. Ind. Appl.*, vol. 55, no. 6, pp. 6517–6526, 2019.
10. N. Campagna, M. Caruso, V. Castiglia, R. Miceli, and F. Viola, "Energy Management Concepts for the Evolution of Smart Grids," *8th International Conference on Smart Grid (icSmartGrid)*, Paris, France, 2020.
11. U. Zafar, S. Bayhan, and A. Sanfilippo, "Home energy management system concepts, configurations, and technologies for the smart grid," *IEEE Access*, vol. 8, no. 6, pp. 119271–119286, 2020.
12. B. Wang, P. Dehghanian, and D. Zhao, "Chance-constrained energy management system for power grids with high proliferation of renewables and electric vehicles," *IEEE Trans. Smart Grid*, vol. 11, no. 3, pp. 2324–2336, 2020.
13. S. K. Rathor and D. Saxena, "Energy management system for smart grid: An overview and key issues," *Int. J. Energy Res.*, vol. 44, no. 6, pp. 4067–4109, 2020.
14. X. Hou, J. Wang, T. Huang, T. Wang, and P. Wang, "Smart home energy management optimisation method considering energy storage and electric vehicle," *IEEE Access*, vol. 7, no. 10, pp. 144010–144020, 2019.
15. P. Rajesh, F. H. Shajin, B. M. Chandra, and B. N. Kommula, "Diminishing Energy Consumption Cost and Optimal Energy Management of Photovoltaic Aided Electric Vehicle (PV-EV) By GFO-VITG Approach," *Energy Sources, Part A: Recovery, Utilisation, and Environmental Effects*, vol. 47, no. 1, pp. 11823–11841, 2021.
16. S. A. Hashmi, C. F. Ali, and S. Zafar, "Internet of Things and cloud computing-based energy management system for demand side management in smart grid," *Int. J. Energy Res.*, vol. 45, no. 1, pp. 1007–1022, 2020.
17. M. Meliani, A. E. Barkany, I. E. Abbassi, A. M. Darcherif, and M. Mahmoudi, "Energy management in the smart grid: State-of-the-art and future trends," *Int. J. Eng. Bus. Manage.*, vol. 13, no. 7, pp. 1–26, 2021.
18. A. Ahmadi, A. Tavakoli, P. Jamborsalamati, N. Rezaei, M. R. Miveh, F. H. Gandoman, A. Heidari, and A. E. Nezhad, "Power quality improvement in smart grids using electric vehicles: A review," *IET Electr. Syst. Transp.*, vol. 9, no. 2, pp. 53–64, 2019.
19. Y. Ma and B. Li, "Hybridised intelligent home renewable energy management system for smart grids," *Sustainability*, vol. 12, no. 5, p. 2117, 2020.
20. F. Delfino, G. Ferro, M. Robba, and M. Rossi, "An energy management platform for the optimal control of active and reactive powers in sustainable microgrids," *IEEE Trans. Ind. Appl.*, vol. 55, no. 6, pp. 7146–7156, 2019.
21. M. A. Khan, N. Gupta, R. Kathuria, S. Vanshika, V. Sharma, and A. K. Vaghmare, "Electric vehicle integration system for power management on a blockchain-based smart grid platform with AI capabilities," 2023, Available: <https://www.researchsquare.com/article/rs-2646860/v1> [Accessed by 09/09/2024].
22. P. Razmjoui, A. Kavousi-Fard, T. Jin, M. Dabbaghjamesh, M. Karimi, and A. Jolfaei, "A blockchain-based mutual authentication method to secure the electric vehicles' TPMS," *IEEE Trans. Ind. Inf.*, vol. 20, no. 1, pp. 158–168, 2023.
23. A. J. Cabrera-Gutiérrez, E. Castillo, A. Escobar-Molero, J. Cruz-Cozar1, D. P. Morales, and L. Parrilla, "Blockchain-based services implemented in a microservices architecture using a trusted platform module applied to electric vehicle charging stations," *Energies*, vol. 16, no. 11, p. 4285, 2023.
24. P. Bhattacharya, S. Tanwar, U. Bodkhe, A. Kumar, and N. Kumar, "EVBlocks: A blockchain-based secure energy trading scheme for electric vehicles underlying 5G-V2X ecosystems," *Wireless Pers. Commun.*, vol. 127, no. 3, pp. 1943–1983, 2022.
25. M. U. Javed, N. Javaid, M. W. Malik, M. Akbar, O. Samuel, A. S. Yahaya, and J. B. Othman, "Blockchain-based secure, efficient and coordinated energy trading and data sharing between electric vehicles," *Cluster Comput.*, vol. 25, no. 3, pp. 1839–1867, 2022.
26. A. F. M. S. Akhter, T. Z. Arnob, E. B. Noor, S. Hizal, and A. S. K. Pathan, "An edge-supported blockchain-based secure authentication method and a cryptocurrency-based billing system for P2P charging of electric vehicles," *Entropy*, vol. 24, no. 11, p. 1644, 2022.

27. S. Tanwar, R. Kakkar, R. Gupta, M. S. Raboaca, R. Sharma, F. H. Alqahtani, and A. Tolba, "Blockchain-based electric vehicle charging reservation scheme for optimum pricing," *Int. J. Energy Res.*, vol. 46, no. 11, pp. 14994–15007, 2022.
28. D. Yang, H. Liu, M. Li, and H. Xu, "Data-driven analysis of battery electric vehicle energy consumption under real-world temperature conditions," *J. Energy Storage*, vol. 72, no. 11, p. 108590, 2023.
29. Y. Dai, T. Chen, G. Wang, and D. Robinson, "An adaptive half-space projection method for stochastic optimisation problems with group sparse regularisation," *Trans. Mach. Learn. Res.*, 2023, Available: <https://openreview.net/forum?id=KBhSyBBeeO> [Accessed by 01/09/2024].
30. A. L. DaViera, M. Uriostegui, A. Gottlieb, and O. C. Onyeka, "Risk, race, and predictive policing: A critical race theory analysis of the strategic subject list," *Am. J. Community Psychol.*, vol. 73, no. 1-2, pp. 91-103, 2023.
31. A. Benhammou, M. A. Hartani, H. Tedjini, H. Rezk, and M. Al-Dhaifallah, "Improvement of autonomy, efficiency, and stress of fuel cell hybrid electric vehicle system using robust controller," *Sustainability*, vol. 15, no. 7, p. 5657, 2023.
32. Z. Wang, W. Luo, S. Xu, Y. Yan, L. Huang, J. Wang, W. Hao, and Z. Yang, "Electric vehicle lithium-ion battery fault diagnosis based on multi-method fusion of big data," *Sustainability*, vol. 15, no. 2, p. 1120, 2023.
33. J. A. Bala, S. A. Adeshina, and A. M. Aibinu, "Performance evaluation of You Only Look Once v4 in road anomaly detection and visual simultaneous localisation and mapping for autonomous vehicles," *World Electr. Veh. J.*, vol. 14, no. 9, p. 265, 2023.